Early photoluminescence decay in *a*-Si:H

D. G. Stearns*
Department of Applied Physics, Stanford University, Stanford, California 94305
(Received 21 February 1984)

Photoluminescence (PL) decay in *a*-Si:H has been measured in the time regime of 0.5—40 nsec, and the dependence upon temperature, emission energy, and excitation energy has been systematically investigated. The subnanosecond time resolution was achieved by using a single-photon—counting detection system in conjunction with synchrotron radiation as the light source. We present an analysis method for quantitatively characterizing the PL decay in terms of a model function, with which the experimental broadening is removed by deconvolution. Deconvoluted PL decay measured at different emission energies is rearranged to yield the time-resolved PL emission spectrum. The behavior of the PL emission spectrum, and the variations of the decay with temperature, emission energy, and excitation energy, provide much insight into the recombination kinetics of photogenerated electron-hole pairs on the nanosecond time scale. The experimental results are interpreted in terms of specific physical processes.

I. INTRODUCTION

In the last decade there has been an extensive scientific effort to study the electronic structure of the amorphous semiconductor *a*-Si:H. This is largely due to the increasing use of *a*-Si:H in cost-effective semiconductor products such as photovoltaic devices. A salient feature of the electronic structure of *a*-Si:H is the existence of an intrinsic distribution of localized electronic states, described as band tails, which strongly influence the electronic transport properties. A valuable source of information about the band-tail states has been the study of photoluminescence (PL).

There have been many previous investigations of PL in *a*-Si:H. We refer the reader to a comprehensive review of the literature by Street.[1] Time-resolved PL studies[2–11] indicate that the decay processes in *a*-Si:H are quite complicated, involving both the radiative and nonradiative recombination of electrons and holes. At low excitation densities ($<10^{18}$ cm^{-3}) the electrons and holes are observed to interact as pairs.[2] The origin and nature of the electron-hole—pair states, however, is not yet fully understood. There is some controversy as to whether the pairs are geminate.[12–14] It has also been suggested that some of the pairs exist as bound excitons[11,15,16]. In order to address these issues, it is important to study the kinetics of the electrons and holes at early times. To this purpose, there has been a considerable effort to measure PL decay in *a*-Si:H with the best possible time resolution. Most of the previous studies have been limited to experimental temporal resolutions of greater than $\sim$10 nsec. Recently, however, there have been several reports of PL decay measurements with subnanosecond time resolution. Wilson *et al.*[11,15] have measured the decay of the integrated PL emission spectrum with a time resolution of $\sim$250 psec. There have also been some preliminary reports[17,18] of energy-resolved PL decay measurements with subnanosecond time resolution.

In this paper we present a study of PL decay in *a*-Si:H during the first 40 nsec after excitation, with an experimental temporal resolution of 500 psec. We have investigated the dependence of the PL decay on emission energy, excitation energy, and temperature. The purpose of this experiment was to perform an energy-resolved study of PL decay in order to investigate the evolution of the electron-hole—pair population within the band-tail states on a nanosecond time scale. All of the measurements in this investigation have been made at low excitation intensities, where the density of excitations never exceeded 10^{16} cm^{-3}. This is well within the monomolecular recombination regime, which allows the results to be safely interpreted in terms of a population of noninteracting electron-hole pairs. The low sensitivity of our detection system in the infrared region has constrained this study of PL decay to emission energies greater than 1.4 eV.

In Sec. II we describe the experimental method used to make the PL decay measurements. The analysis procedure is explained in Sec. III, where we propose a new method for quantitatively characterizing the early decay data. The experimental results are presented in Sec. IV, and the physical implications of these results are discussed in Sec. V. In Sec. VI we present our conclusions.

II. EXPERIMENTAL METHOD

Time-resolved PL decay has been measured in samples of *a*-Si:H made at the Palo Alto Research Center (PARC) of the Xerox Corporation. The samples are approximately 1-μm-thick films produced by the glow-discharge decomposition of 100 vol % silane (SiH_4) gas. The deposition of the films was at high substrate temperature and low power, conditions that have been shown to produce *a*-Si:H with the lowest density of states in the pseudo band gap.[1,19,20] Three samples have been studied, which were chosen for their high PL quantum efficiency. The PL decay exhibited by the three samples is very similar. For the sake of internal consistency and comparison, all of the data presented in this report correspond to one of

these samples. This particular sample was deposited onto a frosted Corning 7059 glass substrate at 230 °C and 2 W rf power. The front surface was subsequently roughened in order to reduce reflection and thin-film interference effects. The optical band gap of this sample was measured to be 1.65 eV.[21] The spin density, which is generally associated with the density of dangling-bond defects, has been shown to be less than 10^{16} cm^{-3} in samples prepared under identical deposition conditions.[22] It is important to emphasize that the type of a-Si:H made at PARC has been exceedingly well characterized and studied.[19,22,23] This makes it possible to directly connect our results with previous investigations, such as the time-resolved PL measurements of Tsang and Street.[2]

The excitation light used in this experiment was synchrotron radiation as provided by the Stanford Synchrotron Radiation Laboratory (SSRL). The synchrotron radiation has an intrinsic temporal structure consisting of pulses of ~200 psec duration [full width at half maximum (FWHM)] at a repetition rate of 1.28 MHz. This experiment was performed in the "Lifetimes Port" facility at SSRL, where synchrotron radiation is available in a continuously tunable energy range of 1—5 eV. In comparison with standard laboratory lasers, the synchrotron is a very weak light source. The peak power output into a 10% spectral bandwidth in the visible spectrum was ~1 mW.

A schematic diagram of the experimental configuration is shown in Fig. 1. The highly collimated synchrotron-radiation beam was extracted through the floor of the Lifetimes Port facility and was reflected into the plane of the optical bench. A small portion of the beam was used to monitor the light intensity, and the remaining beam was reflected by a cold mirror [labeled (3)] into the sample chamber. The light beam passed through a lens [labeled (4)] (the cross section of the beam at this point was approximately 2×3 cm), and was focused to a 1-mm^2 spot on the surface of the sample. Between the lens and the sample was a broadband (40 nm FWHM) interference filter [labeled (5)] that was used to select the excitation energy. The sample was housed in a helium cryostat, where the temperature could be varied between 11 and 300 K. The PL was collected in reflection geometry with a pair of lenses [labeled (6) and (7)], and a 720-nm cutoff filter [labeled (8)] was used to eliminate excitation light scattered off the surface of the sample. The PL emission energy was analyzed with a single-grating, $\frac{1}{4}$-m optical monochromator operating with an energy resolution of 8 nm FWHM.

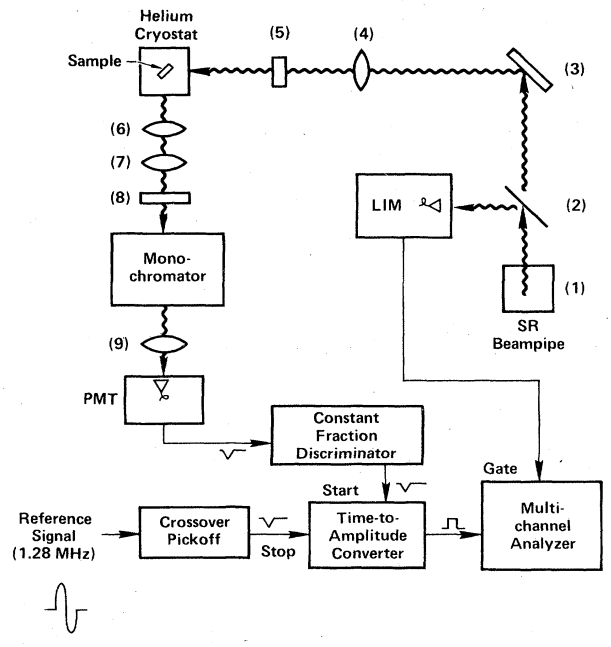

FIG. 1. Schematic diagram of the experimental configuration.

Subnanosecond time resolution was achieved by using the technique of single-photon counting. The output of the monochromator was focused onto a RCA 8852 photomultiplier tube, which is specifically designed for photon-counting applications. The sensitivity of the cesium-doped multialkali cathode decreases exponentially below 1.4 eV, and this defined the low-energy limit of the PL decay measurements. The photomultiplier tube was thermoelectrically cooled in order to minimize the dark-count signal. The pulse out of the photomultiplier tube was sent through a constant-fraction discriminator, which triggered a time-to-amplitude converter. The converter measured the time interval between the arrival of the photon count and a reference pulse that was synchronous with the excitation frequency of 1.28 MHz. A precise reference was obtained from the signal induced by the circulating electron bunch in a small wire coil that was located inside the storage-ring beam pipe. The analog time output from the time-to-amplitude converter was collected in a multichannel analyzer.

There are two conditions that must be satisfied in order for the single-photon—counting technique to function properly. First, it must be realized that for each excitation of the sample, at most one photon can be counted, and this is necessarily the first photon that is detected. An unbiased data set is achieved only when there is a negligible probability that two photons will arrive during the same excitation period. Hence, in order to avoid the phenomenon known as "pile up," where the collection of counts is biased toward earlier times, the counting rate must be kept much smaller than the excitation frequency. A standard criterion used in single-photon counting is that approximately one photon should be detected for every 100 excitations of the sample. This set an upper limit for the counting rate of about 10^4 counts/sec. Calibrated neutral-density filters were used whenever it was necessary to attenuate the PL signal.

The other potential problem with single-photon counting is that the data represent a superposition of PL decay at different times. In other words, some of the counts that are collected correspond to the PL decay from previous excitation pulses and not necessarily the most recent excitation pulse. Then, in order to obtain accurate data with this technique, the PL decay associated with previous excitations must be either negligible or at least constant over the time interval of interest. In the case of a-Si:H, the PL intensity from the previous excitations

(> 780 nsec earlier) is weak (less than 10% of the initial intensity) and is virtually constant over the 40-nsec interval measured in this experiment. This is evident from PL decay measured in the later time regime by various groups.[2–5] Hence the PL contribution from previous excitations of the sample was manifested as a flat background and could be easily removed.

There were two major sources of timing error in this experiment. These were the "jitter" in the photomultiplier-tube output pulse and the instability of the photon-counting electronics. Phototube jitter corresponds to variations in the shape of the leading edge of the output pulse. The jitter was observed to produce a timing error of ~400 psec, and the instability of the electronics contributed an additional timing error of ~100 psec. Thus the total time resolution of the single-photon—counting system, including detection and time conversion, was approximately 500 psec.

A temporal profile of the excitation-light pulse was measured at the beginning of each experimental run. This was accomplished by removing the excitation filter and detecting light that was scattered from the surface of the sample. The excitation-light pulse was measured at room temperature in order to eliminate any PL signal. The sample was subsequently cooled and PL decay data sets were collected. It was necessary to monitor the excitation-light intensity throughout the experimental run, since the intensity was continuously decreasing as the current in the storage ring decayed. The acquisition time for a data set was adjusted so that each data set was normalized to the same integrated light flux incident on the sample. In this way the relative intensity of data sets measured at different times could be accurately compared.

On several occasions in this experiment a continuous-wave (cw) light source was used instead of synchrotron radiation. The cw illumination was provided by a tungsten lamp that simulated a known blackbody emission spectrum. In particular, the tungsten lamp was used to calibrate the energy response of the detection system. The relative energy response of the detection system is required in order to reconstruct the time-resolved PL emission spectrum from PL decay measured at different emission energies. It was found to be very important to measure the detection-system response carefully, as small errors can lead to anomalous structure in the PL emission spectra.

A more detailed description of the experimental apparatus and procedure is available elsewhere.[24]

III. DATA ANALYSIS

The major part of this investigation consisted of collecting a series of PL decay data sets as either the excitation energy, the emission energy, or the temperature was systematically varied. A representative PL decay data set, measured at 20 K with an excitation energy of 2.07 eV and at an emission energy of 1.53 eV, is presented in Fig. 2. The dashed line in this figure represents the experimentally measured excitation-light pulse. The time interval was adjusted so that there were approximately 3 nsec of data before excitation occurred, which could be used to establish the background level. The major sources of the flat background were photomultiplier-tube dark counts and PL arising from previous excitation pulses (see Sec. II). The background level was determined by averaging the pre-excitation signal, and then was removed by subtracting this constant from each channel. The background has been removed from the data set shown in Fig. 2.

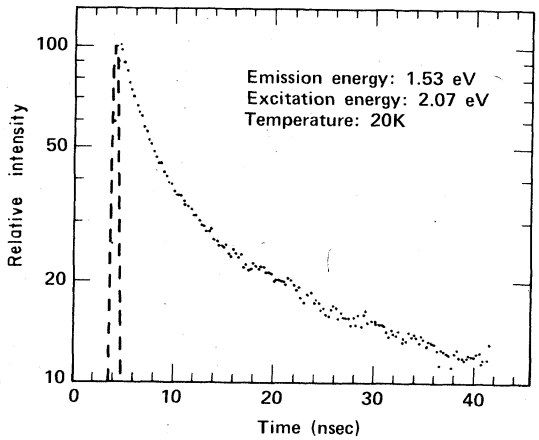

FIG. 2. Representative PL decay data set in which the flat background has been removed. The dashed line is the experimentally measured excitation-light pulse.

The PL decay in Fig. 2 is presented on a logarithmic intensity scale. The significant curvature indicates that the decay is nonexponential in the first 40 nsec. The first few nanoseconds of the same data set are shown in Fig. 3. The PL decay still exhibits curvature on this expanded time scale, and we conclude that the decay is nonexponential up to the earliest times resolvable in this experiment. This nonexponential decay is in direct contrast to the decay of the integrated PL emission spectrum, which has been shown to be nearly exponential in the first 5 nsec after excitation.[11,15] The discrepancy demonstrates that the two measurements provide different information. The decay of the integrated emission spectrum relates to

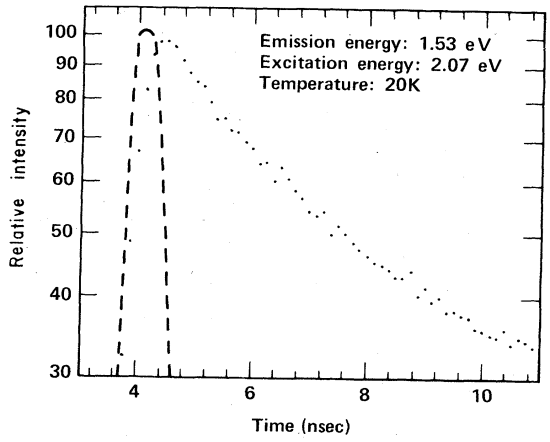

FIG. 3. PL decay data set and excitation-light pulse on an expanded time scale.

changes in the average configuration of the entire electron-hole—pair population. The PL decay measured in this experiment, however, is sensitive to changes in the subpopulation of pairs that occupy states at a particular emission energy. The decay that we measure can include fast nonradiative components that correspond to transitions within the manifold of excited states.

The first step in analyzing the PL decay is to identify the type of recombination kinetics. It has been generally observed that when the density of excitations is less than 10^{18} cm^{-3} the decay kinetics are monomolecular.[1] The manifestation of monomolecular decay is that the shape of the PL decay is independent of excitation intensity. All of the measurements in this experiment have been conducted at low excitation intensity, where the excitation density was less than 10^{16} cm^{-3}, in order to achieve the monomolecular recombination regime. We felt that it was important, however, to verify that the recombination kinetics were monomolecular at early times and under the conditions of this experiment. PL decay was measured as the excitation intensity was varied over 2 orders of magnitude by using calibrated neutral-density filters. The measurements were made at a temperature of 20 K with an excitation energy of 2.33 eV, and all of the detectable PL was collected. (This comprised an emission-energy range of $\sim$1.4—1.6 eV.) It was found that the intensity of the PL decay was linearly proportional to the excitation intensity *at all times* within the 40-nsec range of this experiment, which establishes that the decay kinetics are indeed monomolecular at early times.

Being in the monomolecular regime is extremely important as it indicates that the electrons and holes recombine as noninteracting pairs. In fact, at the typical excitation densities used in this experiment, the average distance between excitations is on the order of 1000 Å. The concept of electron-hole pairs that evolve independently in time simplifies the analysis of the PL decay measurements in the following important way. Since the recombination processes do not involve interactions between electron-hole pairs, the evolution of a pair is independent of the time at which it was created. Then it is physically meaningful to treat the PL decay as the superposition of decay from a distribution of δ-function excitations. The excitation pulse can be deconvoluted out of the PL decay, yielding the decay response to a single δ-function excitation. The deconvoluted PL decay exhibits the physical characteristics of interest, while the experimental broadening due to the shape of the excitation pulse and the response of the detection system has been removed.

It has been shown that the PL decay at a particular emission energy is nonexponential, even in the first few nanoseconds after excitation. A natural explanation of this nonexponential behavior is that there exists a distribution of decay rates. This distribution arises because the electron-hole pairs are expected to occupy many different types of states in the disordered a-Si:H system. For the purpose of comparing the PL decay data in a quantitative way, it was desirable to establish a method of characterizing the distribution of decay rates.

An obvious possible technique for extracting a decay time from the data is to approximate the earliest decay with a single exponential. This approach has two distinct disadvantages. First, there is inherent ambiguity, as the decay time that is determined will depend upon the interval of time that has been used in the approximation. Second, the experimentally measured decay, particularly in the first few nanoseconds, is not strictly the decay response of the sample, but is instead the convolution of the decay response with the shape of the excitation pulse and the response of the detection system. The sharp features of the intrinsic decay become broadened, so that the decay time determined from the slope of the experimental data is expected to be overestimated.

We now present an alternate method for quantitatively analyzing the PL decay at early times. This method was designed to explicitly remove the effects of experimental broadening and thus characterize the intrinsic decay response.

A. Model function

When the PL decay in a-Si:H is treated as a superposition of many decay rates, it is found that the fastest decay components, which dominate on the time scale of this experiment, are actually relatively weak. This can be seen in the decay time distribution derived by Tsang and Street from PL decay in the time regime of 10^{-8}—10^{-2} sec (see Ref. 2, p. 3030). They found that the distribution actually peaks at $\sim 10^{-4}$ sec, and is largely attenuated at 10^{-6} sec. Thus we conclude that the decay rates that are important in the time regime of this experiment (0.5—40 nsec) are in the tail of the distribution of decay rates, well removed from the peak of the distribution.

We now proceed to model the tail of the decay rate distribution and derive a simple analytical expression for PL decay. The derivation relies upon an important property of any function that is expressed as a superposition of exponential decays: The behavior of the function at a particular time t_0 is determined by the decay components that correspond to decay times close to t_0. The explanation of this phenomenon is simple. Decay components much earlier than t_0 have died out, and components much later than t_0 contribute a constant background. Thus by modeling the tail of the decay rate distribution, the early decay can be reconstructed without any knowledge of the distribution in a later time regime.

Let $I(t)$ represent the PL decay at emission energy $E_{\rm em}$ that results from a δ-function excitation pulse. Then the PL decay measured in this experiment would be the convolution of $I(t)$ with the experimentally measured excitation pulse. We express $I(t)$ as a superposition of exponential decays,

$$I(t)=\int_0^\infty \nu_r F(\nu)\exp(-\nu t)d\nu\,, \tag{1}$$

where ν is the decay rate related to the decay time τ by

$$\nu=1/\tau\,, \tag{2}$$

and ν_r is the average radiative recombination rate for electron-hole pairs that have a total decay rate of ν. It is important to point out that the distribution function $F(\nu)$ *is not* strictly the distribution of decay rates. This is because the decay kinetics are actually very complicated.

There are three general types of channels through which the electron-hole—pair population at energy E_{em} can change. Two of these, radiative recombination and nonradiative transitions into lower-energy states, represent decay processes that deplete the population of pairs at E_{em}. The third type of channel corresponds to the nonradiative transition of pairs into states at energy E_{em} from higher-energy states. These channels feed into the electron-hole—pair states at E_{em}, which couples the population of pairs at E_{em} to the pair populations at all higher energies. Thus it is not rigorously correct to treat the PL decay problem in terms of an initial population of pairs that is depleted by a distribution of decay rates, as is represented in Eq. (1).

In our analysis of PL decay we will ignore the possibility that the pair population at E_{em} is being fed by populations at higher energies, so that we can interpret $F(\nu)$ as the distribution of decay rates. This is justified to some extent by the observation that the energy range studied in this experiment corresponds to the high-energy portion of the PL emission spectrum. At these emission energies, the channels feeding into the pair population at E_{em} are less important, since there are relatively few electron-hole pairs at energies greater than E_{em}.

Next we assume that the distribution of decay rates $F(\nu)$ falls off exponentially for large ν. There is no particular physical motivation for modeling the tail of the decay rate distribution as an exponential; this choice was the result of trying several different possible functional representations, where it was found empirically that the exponential representation best reproduced the measured PL decay. Then,

$$\nu_r F(\nu)=a_2\exp(-\tau_0\nu)\ ,\quad \nu\rightarrow\infty \tag{3}$$

where a_2 is a constant and we have neglected any comparatively weak algebraic ν dependence.

Our purpose is to model PL decay which extends over the time regime $0<t<t_m$, where $t_m\simeq 40$ nsec. Equation (1) is rewritten as

$$I(t)=\int_0^{\bar{\nu}}\nu_r F(\nu)e^{-\nu t}d\nu+\int_{\bar{\nu}}^{\infty}\nu_r F(\nu)e^{-\nu t}d\nu\ , \tag{4}$$

where $\bar{\nu}$ is chosen to satisfy the following two criteria:

(1) $\bar{\nu}t_m\ll 1$;
(2) $\nu_r F(\nu)=a_2\exp(-\tau_0\nu)$ over the interval $\bar{\nu}<\nu<\infty$.

A reasonable value of $\bar{\nu}$ that would satisfy these criteria is $\bar{\nu}\sim 10^6\ \text{sec}^{-1}$. Now, in the time regime of the PL decay measured in this work, we have

$$\exp(-\nu t)\simeq 1,\quad 0<\nu<\bar{\nu}\ . \tag{5}$$

Then the first integral in Eq. (4) can be simplified, and, in the second integral, $\nu_r F(\nu)$ is replaced to obtain

$$\begin{aligned} I(t)&=\int_0^{\bar{\nu}}\nu_r F(\nu)d\nu+\int_{\bar{\nu}}^{\infty}a_2\exp[-\nu(t+\tau_0)]d\nu \\ &=\int_0^{\bar{\nu}}\nu_r F(\nu)d\nu+\frac{a_2\exp[-\bar{\nu}(t+\tau_0)]}{t+\tau_0}\ . \end{aligned} \tag{6}$$

It will be seen that τ_0 is at most a few nanoseconds, so that the exponential in (6) is well approximated by unity. The first term is a constant,

$$a_1\equiv\int_0^{\bar{\nu}}\nu_r F(\nu)d\nu\ . \tag{7}$$

Thus we arrive at the simple analytical expression for PL decay at early times,

$$I(t)=a_1+\frac{a_2}{t+\tau_0}\ . \tag{8}$$

Equation (8) is the model function that we have used in analyzing experimentally measured PL decay. It has been derived solely on the premise that the tail in the decay rate distribution for the range $\nu\geq 10^6\ \text{sec}^{-1}$ can be approximated with an exponential.

At this point it is useful to consider the physical meaning of the parameters that appear in the model function (8). The initial PL intensity can be expressed as

$$I(0)=a_1+a_2/\tau_0\ . \tag{9}$$

By referring to Eq. (6) it is apparent that the parameter a_1 represents the contribution to the initial PL intensity from the electron-hole pairs that decay at rates slower than $\bar{\nu}$. Hence the quantity $a_1\tau_0/a_2$ has a physical significance as the fractional contribution to the early PL decay from the slow decay components ($\nu<\bar{\nu}$) in the decay rate distribution.

The other physically meaningful quantity is τ_0, which we call the "decay time cutoff." This parameter represents how fast the decay rate distribution attenuates at large ν, and thus characterizes the strength of the fast decay components. There is a simple analytical interpretation of the decay time cutoff τ_0 which is valid when the quantity $a_1\tau_0/a_2$ is small, such that

$$a_1\tau_0/a_2\ll 1\ . \tag{10}$$

It will be shown in the following section that condition (10) was always satisfied for the PL decay measured in this experiment. Then for very early times, the model function (8) can be approximated by

$$I(t)\simeq\frac{a_2}{t+\tau_0},\quad t\simeq 0\ . \tag{11}$$

Next we take the time derivative of the logarithm of the intensity $I(t)$ and obtain

$$\left[\frac{d}{dt}\ln I(t)\right]_{t=0}=-1/\tau_0\ . \tag{12}$$

Thus the quantity $-1/\tau_0$ can be identified as the initial slope of the deconvoluted PL decay, when it is plotted on a semilogarithmic scale.

B. Deconvolution

The analysis of the PL decay consisted of deconvoluting the data by assuming that the decay response to a δ-function excitation was of the form of Eq. (8). The deconvolution was accomplished by numerically convoluting the model function (8) with the experimentally measured excitation-light pulse. The result was fit to a PL decay data set by using a minimization routine that searches

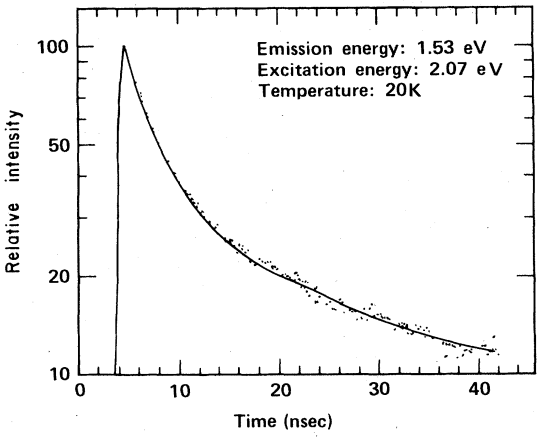

FIG. 4. Best analytical fit to the PL decay data set shown in Fig. 2, using the model function (8).

the parameter space of the model function. The values of the parameters that best reproduced the experimental data were then used to generate the deconvoluted PL decay according to the model function. The deconvolution procedure is discussed in more detail in the Appendix.

The PL decay data set shown in Fig. 2 is presented again in Fig. 4, along with the best fit generated using the model function (8). The fit is excellent over the entire data set, which indicates that the model function is a good representation of the decay in this time regime. The corresponding deconvoluted PL decay is presented in Fig. 5. The values of the decay time cutoff τ_0 and $a_1\tau_0/a_2$ derived from this data set are $\tau_0=1.56$ nsec and $a_1\tau_0/a_2=0.55$.

Several hundred PL decay data sets have been analyzed using the procedure described in this section, and the model function (8) has consistently generated excellent fits to the data. The quantity $a_1\tau_0/a_2$ was always found to be small, corresponding to at most a few percent of the initial PL intensity. Values of the decay time cutoff τ_0 ranged from ~ 5 nsec to being immeasurably small. A discussion of error analysis, including the estimation of error limits in the parameters a_1, a_2, and τ_0, is given in the Appendix.

IV. EXPERIMENTAL RESULTS

A. Emission-energy dependence

The behavior of PL decay in a-Si:H was observed to vary significantly with the emission energy. An example of deconvoluted PL decay measured at different emission energies is exhibited in Fig. 6. These data were taken at 20 K using an excitation energy of 2.07 eV. The decay curves have been normalized to facilitate comparison. In particular, it is evident that the average decay rate increases as the emission energy increases. By analyzing the decay in terms of the model function (8), we have obtained values for the quantities τ_0 and $a_1\tau_0/a_2$ as a function of emission energy. These values are listed in Table I. The decay time cutoff τ_0 and the quantity $a_1\tau_0/a_2$ directly relate to the decay rate distribution characteristic of the nonexponential PL decay. The trend towards smaller decay time cutoffs and smaller values of $a_1\tau_0/a_2$ with higher emission energy is indicative of an increase in the relative strength of the fast decay components.

PL decay data such as those shown in Fig. 6 have been rearranged in order to construct the time-resolved PL emission spectrum. A set of emission spectra, corresponding to times ranging from 0.5 to 20 nsec, is presented in Fig. 7. The emission spectrum in the first 40 nsec is found to be a single broad peak. The solid lines in Fig. 7 are Gaussian fits to the data, demonstrating that the emission spectrum is well approximated by a Gaussian line shape at early times. In particular, we find no evidence of a second, higher-energy peak in the emission spectrum, as was previously reported.[5]

The time-resolved emission spectrum exhibits two important features. First, it is observed that there is a large amount of attenuation on the nanosecond time scale. The amplitude of the emission spectrum decreases by $\sim 70\%$ in the first 20 nsec. The second feature is a significant translation of the emission spectrum to lower energy with time. It is conventional to characterize this shift by

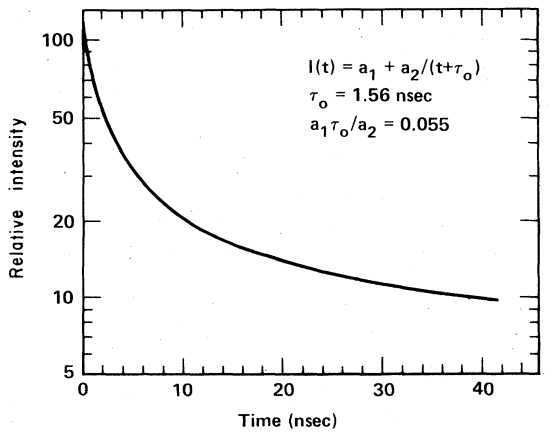

FIG. 5. Deconvoluted PL decay derived from the data set shown in Fig. 2.

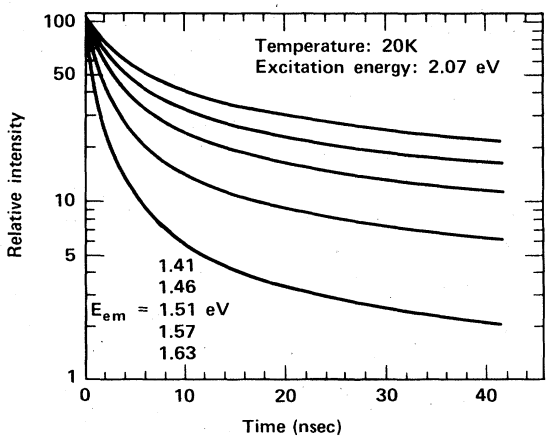

FIG. 6. Deconvoluted PL decay corresponding to different emission energies. These curves have been normalized to 100.

TABLE I. Values of the decay time cutoff τ_0 and the quantity $a_1\tau_0/a_2$ at different emission energies, derived from PL decay measured at a temperature of 20 K and with an excitation energy of 2.07 eV.

E_{em} (eV)	τ_0 (nsec)	$a_1\tau_0/a_2$
1.39	5.65±1.52	0.13 ±0.09
1.41	4.41±0.81	0.14 ±0.07
1.43	4.00±0.51	0.14 ±0.04
1.44	3.28±0.35	0.12 ±0.03
1.46	2.93±0.26	0.11 ±0.02
1.48	2.53±0.21	0.091±0.017
1.49	2.23±0.18	0.080±0.014
1.51	1.93±0.15	0.066±0.012
1.53	1.56±0.13	0.055±0.010
1.55	1.18±0.11	0.040±0.008
1.57	0.95±0.11	0.029±0.006
1.59	0.71±0.10	0.020±0.005
1.61	0.45±0.10	0.011±0.004
1.63	0.26±0.11	0.004±0.003
1.65	0.14±0.12	0.000±0.001

measuring the time dependence of the peak of the emission spectrum. The time-resolved shift of the peak position in the first few nanoseconds after excitation (as determined from the Gaussian fits) is presented in Fig. 8. The rate at which the peak shifts is found to be ~0.04 eV per decade of time. This behavior is consistent with an extrapolation of the emission peak shift in the time regime of 10^{-6}–10^{-8} sec observed by Tsang and Street in similar samples (see Ref. 2, p. 3031).

B. Temperature dependence

It is a well-established phenomenon that PL in *a*-Si:H is quenched at temperatures greater than ~50 K.[1] It has been previously observed[25] that the temperature dependence of the cw PL intensity I_{cw} obeys the empirical relationship,

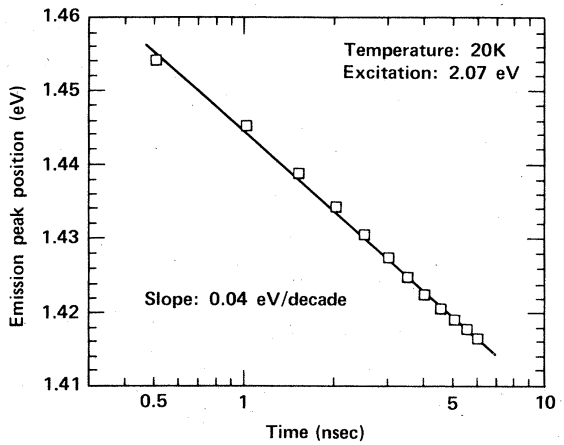

FIG. 8. Time-resolved shift of the peak of the PL emission spectrum in the first few nanoseconds after excitation.

$$1/I_{cw}=1/I_0+B\exp(T/T_0)\,, \tag{13}$$

where the parameter T_0 is universally found to be ~23 K. We have measured the cw PL intensity as a function of temperature at two emission energies, 1.43 and 1.53 eV. The results corresponding to 1.43 eV are presented in Fig. 9. The solid line represents the best fit of Eq. (13) to the data. We have found that the temperature dependence of the cw PL intensity is in excellent agreement with Eq. (13), and the values of the parameter T_0 were determined to be (15.5±0.1) K at 1.43 eV and (16.6±0.2) K at 1.53 eV. We note, however, that the values of T_0 derived in this case are smaller than the "universal" value of 23 K.

The time-resolved PL decay also exhibited a pronounced temperature dependence. PL decay was measured at emission energies of 1.43 and 1.53 eV and at temperatures ranging from 11 to 140 K. The deconvoluted decay measured at 1.43 eV and at several different temperatures is presented in Fig. 10. The salient feature of the temperature dependence of the PL decay is the thermal enhancement of the average decay rate. Analysis

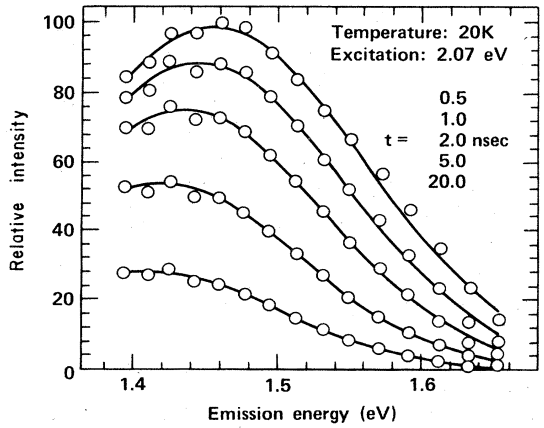

FIG. 7. Time-resolved PL emission spectrum in the first few nanoseconds after excitation. The solid lines represent Gaussian least-squares fits to the data points.

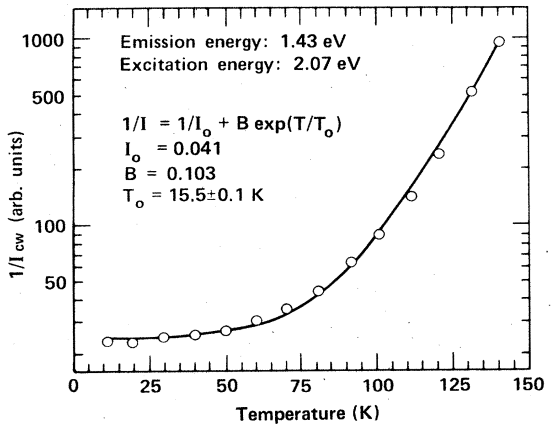

FIG. 9. Temperature dependence of the cw PL intensity at an emission energy of 1.43 eV. The solid line represents the best fit to Eq. (13).

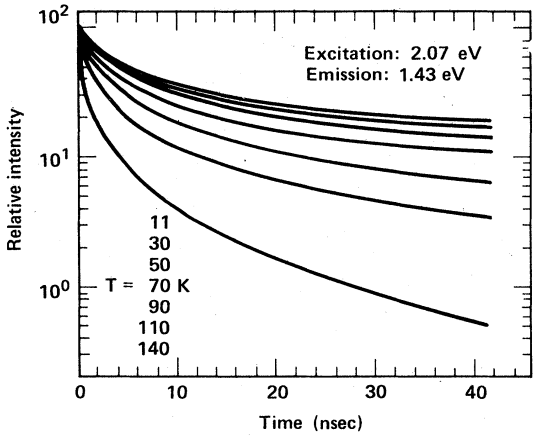

FIG. 10. Deconvoluted PL decay corresponding an emission energy of 1.43 eV and measured at different temperatures. These curves have not been normalized.

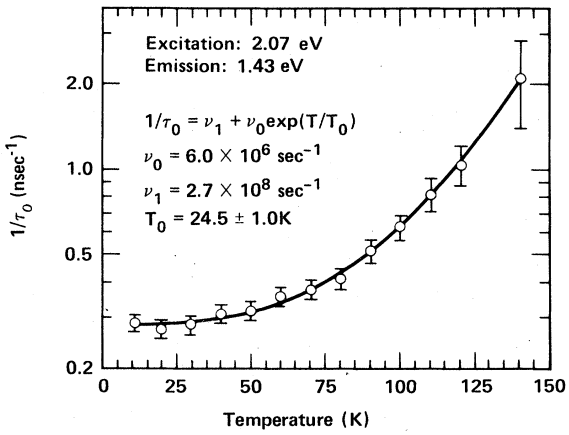

FIG. 11. Temperature dependence of the decay time cutoff τ_0 at an emission energy of 1.43 eV. The solid line represents the best fit to Eq. (14).

of the PL decay has provided values of the decay time cutoff τ_0 and the quantity $a_1\tau_0/a_2$. These values are listed in Table II. Note that both τ_0 and $a_1\tau_0/a_2$ decrease significantly at higher temperature. This indicates that the fast decay components of the decay rate distribution become relatively stronger with increasing temperature.

The values of τ_0 that were derived from PL decay at 1.43 eV are displayed graphically in Fig. 11. It is found that the temperature dependence of τ_0 is well described by the relationship

$$1/\tau_0 = \nu_1 + \nu_0 \exp(T/T_0) \, . \tag{14}$$

The solid line in Fig. 11 represents the best fit of Eq. (14) to the values of τ_0. The parameter T_0 is found to be (24.5±1.0) K at an emission energy of 1.43 eV and (18.5±0.7) K at 1.53 eV. The close similarity between Eqs. (14) and (13) indicates that the decay time cutoff τ_0 and the cw PL intensity have the same temperature dependence. The linear relationship between τ_0 and I_{cw} is exhibited explicitly in Fig. 12. This quantitative correlation demonstrates that the decrease in the cw PL intensity (i.e., the PL efficiency) at higher temperatures is associated with an enhancement of the fast decay components. The thermally enhanced decay is evidently nonradiative in nature.

The data in Fig. 10 depict the relative intensity of the PL decay at different temperatures. An interesting

TABLE II. Values of the decay time cutoff τ_0 and the quantity $a_1\tau_0/a_2$ at different temperatures (T), derived from PL decay measured at emission energies of 1.43 and 1.53 eV. The excitation energy was 2.07 eV.

	T (K)	τ_0 (nsec)	$a_1\tau_0/a_2$
$E_{em}=1.43$ eV	11	3.50±0.25	0.12 ±0.02
	20	3.65±0.26	0.11 ±0.02
	30	3.53±0.25	0.11 ±0.02
	40	3.22±0.25	0.090±0.018
	50	3.15±0.23	0.076±0.017
	60	2.80±0.22	0.059±0.015
	70	2.64±0.21	0.050±0.014
	80	2.42±0.20	0.029±0.012
	90	1.94±0.18	0.017±0.009
	100	1.60±0.16	0.011±0.008
	110	1.23±0.16	0.005±0.006
	120	0.96±0.15	0.000±0.003
	140	0.47±0.15	0.000±0.003
$E_{em}=1.53$ eV	11	1.31±0.07	0.059±0.006
	20	1.31±0.08	0.055±0.006
	30	1.19±0.09	0.044±0.006
	40	1.19±0.08	0.038±0.005
	50	1.12±0.08	0.031±0.005
	60	0.90±0.08	0.023±0.004
	70	0.81±0.07	0.016±0.003
	80	0.72±0.08	0.009±0.003
	90	0.52±0.07	0.005±0.002
	100	0.36±0.06	0.002±0.001
	110	0.22±0.06	0.000±0.001

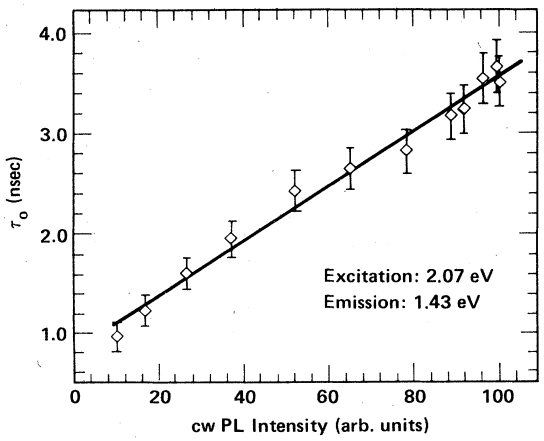

FIG. 12. Demonstration of the linear relationship between the decay time cutoff τ_0 and the cw PL intensity I_{cw} as the temperature is varied. (The data points correspond to different temperatures.)

feature of the decay is that, within experimental resolution, the initial intensity *is independent* of temperature. This behavior was observed at both emission energies investigated. The temperature independence of the initial intensity provides an important insight into the early distribution of the electron-hole pairs among the band-tail states in *a*-Si:H and will be discussed in detail in the next section.

It is also informative to examine the temperature dependence of the time-resolved PL emission spectra. Emission spectra measured at 20, 50, and 80 K are presented in Fig. 13. The spectra correspond to times ranging from 0.5 to 20 nsec. It is apparent that, at any particular time, the emission band occurs at lower energy with increasing temperature. One possible explanation of this temperature dependence is that the width of the pseudo band gap decreases at higher temperatures. Thermally induced changes in the pseudo band gap have been observed in *a*-Si:H.[2] However, the shrinkage of the pseudo band gap is too small to explain the significant difference in the positions of the emission spectra shown in Fig. 13. An alternate explanation is simply, that at higher temperatures, the time-resolved shift of the emission spectrum to lower energy is faster. It is natural to associate the accelerated shift of the emission spectrum with the observed thermal enhancement of the nonradiative-decay components. Specifically, the nonradiative-decay rate at a particular emission energy increases with temperature because the electron-hole pairs are able to relax more rapidly into band-tail states at lower energy.

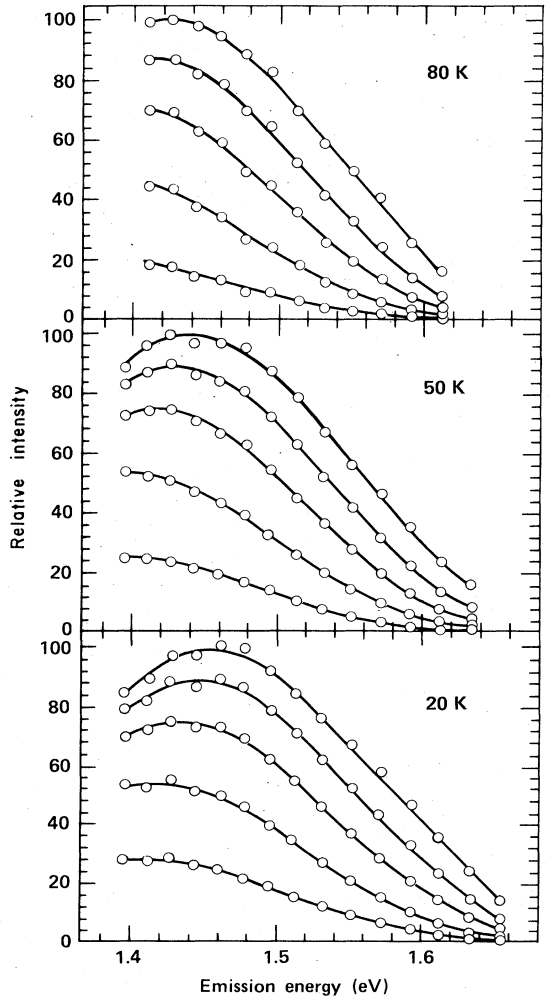

FIG. 13. Time-resolved PL emission spectrum measured at 20, 50, and 80 K. The excitation energy was 2.07 eV. Each set of spectra correspond to times of 0.5, 1.0, 2.0, 5.0, and 20.0 nsec.

C. Excitation-energy dependence

There were found to be small but systematic changes in the PL decay as the energy of the excitation light was varied. A typical example of the excitation-energy dependence is presented in Fig. 14. The PL decay was measured at a temperature of 20 K and an emission energy of 1.48 eV, and the decay curves have been normalized to facilitate comparison. The PL decay corresponds to excitation energies ranging from 1.77 to 2.48 eV. It is evident in Fig. 14 that the effect of increasing the excitation energy is to *decrease* the decay rate. This trend was, in fact, observed at all of the temperatures and emission energies investigated.

The decrease in the average decay rate with increasing excitation energy is in qualitative agreement with the measurements of Shah *et al.*[7] Fischer *et al.*,[26] however, have observed the opposite behavior, namely that the initial decay is faster at higher excitation energy. They propose that the increase in the decay rate can be attributed to nonradiative surface recombination, which is enhanced as the absorption length decreases. In order to investigate the possibility that the excitation-energy dependence is a surface-related phenomenon, we have compared PL decay measured using front illumination to decay measured when the sample was illuminated from the backside (through the glass substrate). It is unlikely that the surface recombination at the front and back surfaces of the *a*-Si:H film would be identical, owing to the physical differences of the interfaces. Then, if the excitation-energy dependence was associated with the density of

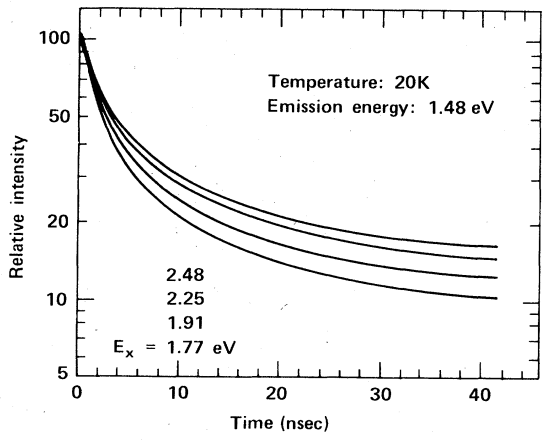

FIG. 14. Deconvoluted PL decay corresponding to different excitation energies. The curves have been normalized to 100.

TABLE III. Values of the decay time cutoff τ_0 and the quantity $a_1\tau_0/a_2$ at different excitation energies, derived from PL decay measured at temperatures of 20, 60, and 100 K. The emission energy was 1.48 eV.

	E_x (eV)	$E_x - E_{em}$ (eV)	τ_0 (nsec)	$a_1\tau_0/a_2$
20 K	1.77	0.29	1.55±0.24	0.057±0.018
	1.91	0.48	1.89±0.11	0.074±0.010
	2.07	0.59	2.10±0.10	0.080±0.009
	2.25	0.77	2.30±0.12	0.092±0.011
	2.48	1.00	2.45±0.20	0.105±0.019
60 K	1.91	0.48	1.53±0.14	0.040±0.009
	2.07	0.59	1.70±0.12	0.043±0.008
	2.25	0.77	2.04±0.16	0.049±0.010
	1.48	1.00	2.19±0.22	0.059±0.015
100 K	1.91	0.48	0.71±0.13	0.006±0.005
	2.07	0.59	0.87±0.11	0.005±0.004
	2.25	0.77	1.01±0.13	0.007±0.005
	2.48	1.00	1.08±0.17	0.006±0.007

electron-hole pairs created near the active surface, one would expect the average decay rate to vary between front and back illumination. There were *no differences* observed between the PL decay measured using front and back illumination. Hence, we conclude that the decrease in the average decay rate with increasing excitation energy is an intrinsic phenomenon of bulk a-Si:H.

The analysis of the PL decay has yielded values of the decay time cutoff τ_0 and the quantity $a_1\tau_0/a_2$ which are listed in Table III. It is seen that the decay time cutoff systematically increases at all temperatures as the excitation energy increases. This indicates that the decay rate distribution contains fewer fast decay components at higher excitation energies.

V. INTERPRETATION

A. Nature of electron-hole pairs

In this section the measurements of PL decay in a-Si:H are interpreted in terms of specific physical processes relating to the kinetics of electron-hole-pairs. We begin by discussing what is meant by an "electron-hole—pair" excitation. It was found that, under the experimental conditions of this investigation, the recombination kinetics associated with PL decay are monomolecular. Monomolecular decay has generally been observed in a-Si:H at low temperatures and low excitation densities, and is considered to be evidence that the photogenerated electrons and holes recombine as noninteracting pairs.

It is useful to explain the difference between an electron-hole pair and an exciton. Consider an eigenstate of the disordered system corresponding to an electron and a hole in the localized band-tail states. Suppose that the electron and the hole can be identified with well-separated regions of space. Then, to a first approximation, the electron and hole can be treated as independent particles that are weakly correlated through the Coulomb interaction. This is an electron-hole pair. The electron and hole occupy localized states with amplitudes that decay exponentially in space. As a result, the overlap of the particles is small and decreases exponentially with the distance between the localized electron and hole.

The other possibility is that the electron and the hole do not exist in well-separated regions of space. Then the positions of the particles are significantly correlated through the Coulomb interaction, and it is inappropriate to consider the particles as occupying independent localized states. In this case, the electron and hole form a bound state as a localized exciton. The overlap of the electron and hole wave functions can be large in an exciton.

Thus the distinction between an exciton and an electron-hole pair depends upon whether the electron and hole can be identified with well-separated regions of space. There is clearly a continuous range of intermediate possibilities where the excitation exhibits both electron-hole—pair and excitonlike features. This should particularly be true for pairs in which the electron and hole are localized on nearby sites. It is likely that electron-hole pairs, excitons, and their hybrids all exist to some extent in a-Si:H. In the following discussion we will tend to suppress the distinction between electron-hole pairs and excitons. All of the photoexcitations will be generically described as electron-hole pairs, except in a few cases where the interpretation of the experimental results specifically requires that a distinction be made.

Although it is evident that electron-hole pairs exist in a-Si:H, there is some controversy as to the origin of the pairs. Tsang and Street[2] propose that the pairs are geminate, that is, an electron and hole that are created when a photon is absorbed remain correlated in space during thermalization and eventually recombine. In contrast, Dunstan[11] argues that the electrons and holes thermalize independently and become distributed randomly in space. In his "distant-pair recombination" model, the occurrence of electron-hole pairs is attributed to arbitrary correlations within the random distributions. The major difference between these models concerns the kinetics of thermalization and, in particular, the diffusion length of the photogenerated particles during thermalization. If the mobilities of the electron and hole are sufficiently low to prevent the particles from separating as they relax into strongly localized states, then the electron-hole pairs will be geminate. If, however, at least one of the particles diffuses over a large distance during thermalization (compared to the average separation between excitations), then the electron-hole pairs will be nongeminate.

B. Average initial separation of an electron-hole pair

We now consider the excitation-energy dependence of the early PL decay, as this relates directly to the issue of geminate recombination. It has been observed that the PL decay changes systematically as the energy of the excitation radiation is varied. In particular, the decay rate cutoff τ_0 increases with excitation energy, which indicates that the distribution of decay times is shifting to longer

times. Shah *et al.*[7] have reported similar behavior for the excitation-energy dependence of the early decay in *a*-Si:H. We adopt their explanation in terms of the average initial separation of the electron-hole pair.

The explanation is based upon a model for the thermalization of photogenerated electron-hole pairs that was first presented by Davis,[27] and was further developed by Knights and Davis.[28] In this model, a photogenerated pair relaxes into the band-tail states by emitting phonons of energy $h\nu_0$ at an average time interval of $1/\nu_0$ seconds. Each emission process is considered to be one step in a random walk. Thus the electrons and holes tend to diffuse into space, so that their relative positions, upon reaching the localized band-tail states, are described by a Gaussian distribution. The width r_0 of this distribution is given by

$$r_0^2=[(E_x-E_{\rm em})+(e^2/4\pi\kappa r_0)](D/h\nu_0^2) . \quad (15)$$

Here, E_x is the excitation energy, $E_{\rm em}$ is the PL emission energy, D is a diffusion coefficient, and κ is the dielectric constant. The term in square brackets represents the total energy lost by an electron-hole pair in the thermalization process. This is clearly a simplified description of a very complex process. The important feature of the model is that it predicts that the initial distribution of electron-hole—pair separations within the localized states is a Gaussian, centered at the origin, with a variance related to the excitation energy. It is not possible to quantitatively apply this model to the observed change in the PL decay rate because the relationship between the recombination rate and the electron-hole separation is unknown.[29] Qualitatively, however, we can assume that the average recombination rate decreases as the width r_0 of the initial distribution increases. Then, as the excitation energy increases, the electron is more likely to be found in a site further away from the hole site, and the decay rate distribution tends to contain slower decay components.

A key feature of this explanation is the assumption that the electron-hole pairs are geminate. Indeed, it is the geminate nature of the pairs that allows the decay rates to be related to the excitation energy. If the electron-hole pairs arise from random spatial distributions, as is asserted in the distant-pair model of recombination, then the distribution of pair separations, and the corresponding distribution of PL decay rates, is expected to be *independent* of excitation energy. Hence, the experimentally observed variation of the early PL decay with excitation energy is evidence that the electron-hole pairs recombining on the nanosecond time scale are geminate.

C. Thermalization of the pair population

The temperature dependence of the PL decay yields important information about the initial distribution of the electron-hole—pair population among the excited states. It was found that the initial PL intensity at a particular emission energy is independent of temperature. In order to investigate this behavior, we write the initial PL intensity $I(0)$ as

$$I(0)=n_0\bar{\nu}_r , \quad (16)$$

where n_0 is the initial population of electron-hole pairs recombining at emission energy $E_{\rm em}$, and $\bar{\nu}_r$ is the average radiative recombination rate of these pairs. It seems improbable that the temperature dependences of n_0 and $\bar{\nu}_r$ would exactly cancel each other. A more plausible explanation of the temperature independence of the initial intensity $I(0)$ is that both $\bar{\nu}_r$ and the initial population of electron-hole pairs n_0 at energy $E_{\rm em}$ are independent of temperature.

Let us consider how a population of electron-hole pairs becomes thermally distributed among the spectrum of excited states. Since recombination to the ground state is a slow process for most of the pairs,[2] then on a picosecond time scale the population will evolve towards a thermal-equilibrium distribution within the manifold of excited states. If the population of electron-hole pairs was able to reach thermal equilibrium within the time resolution of this experiment ($\sim$500 psec), the number of pairs at energy $E_{\rm em}$ would be proportional to a Boltzmann factor $\exp[-(E_{\rm em}-E_0)/kT]$, where E_0 is the energy of the lowest excited state. The exponential Boltzmann factor would imply a very strong temperature dependence on the number of electron-hole pairs recombining at energy $E_{\rm em}$, and, consequently, on the initial PL intensity. Since this is not observed, we conclude that the electron-hole—pair population does not become thermally distributed among the manifold of excited states on a picosecond time scale.

It is evident, however, that photogenerated electron-hole pairs couple strongly to their atomic environment. Time-resolved induced absorption measurements[30] indicate that when electrons and holes are created at an energy exceeding the width of the pseudo band gap (excitation energy of 2.0 eV), they relax into the band-tail states at a rate of $\sim$0.1 eV/psec. This initial relaxation represents the distribution of the electron-hole pairs, within a few picoseconds, among the kinetically *accessible* localized states. That is, the pairs rapidly thermalize into the localized excited states near the positions in space where they were created. This is consistent with the concept of geminate pairs. The electron and hole remain spatially correlated because their low mobility within the localized states inhibits them from separating during the thermalization process. We expect that on a nanosecond time scale the population of electron-hole pairs continues to evolve towards true equilibrium within the entire manifold of excited states, but at a severely reduced rate, due to the small transition rates between the localized states.

D. Kinetics of electron-hole pairs at low temperature

The main purpose of this experiment is to understand the evolution of electron-hole pairs within the band-tail states at early times in *a*-Si:H. Much can be construed from the behavior of the time-resolved PL emission spectrum (Fig. 7). In particular, it has been found that the emission spectrum at 20 K shifts to lower energy and attenuates by $\sim$70% within the first 20 nsec.

The time-resolved shift of the PL emission spectrum has a simple explanation originally due to Tsang and Street.[2] They propose that the shift represents the relaxation of the electron-hole pairs into lower-energy configu-

rations in a continuation of thermalization. This interpretation is consistent with our observation that the electron-hole—pair population is not in thermal equilibrium within the manifold of excited states at early times. The thermalization process can be thought of as a readjustment of the distribution of the pair population among the localized states, as the number of states that is kinetically accessible to each pair increases. The relaxation of the pair population into a lower-energy configuration has been observed explicitly by Wilson *et al.*[15] They found that the PL signal corresponding to emission at energies less than 1.25 eV actually increases during the first nanosecond after excitation, as the population of electron-hole pairs in the low-energy band-tail states builds up.

Further insight into the thermalization process is provided by the PL decay measured at particular emission energies (Fig. 6). The decay at a particular emission energy is sensitive to the depletion of the pair population at that energy due to the thermalization of these pairs into lower-energy states. We observed that the decay is significantly faster at higher emission energies. One possible explanation of this phenomenon is that the electron-hole pairs that recombine at higher emission energy thermalize more rapidly into lower-energy states. This is because the pairs in higher-energy states tend to be less localized,[31] and thus they overlap more states at lower energies into which they can make a transition. An additional explanation is that, since the pairs at higher energy are less localized, they will have more electron-hole overlap and consequently faster recombination rates. Thus we believe that the faster decay at higher emission energies is associated with less localization of the electron-hole pair, which can increase both the thermalization rate and the recombination rate.

The other important feature of the time-resolved PL emission spectrum is the rapid attenuation of the spectrum within the first 20 nsec. Previous measurements of the decay of the integrated emission spectrum have yielded a decay time of ~ 8 nsec.[11,15] We cannot directly integrate the emission spectrum due to the limited energy range of our experiment. However, the attenuation that we observe indicates a comparable decay time for the integrated spectrum.

In order to interpret the behavior of the PL emission spectrum, it is useful to write a simplified expression for the time-dependent intensity $S(t)$ of the integrated emission spectrum,

$$S(t)=\bar{\nu}_r(t)N(t)\ . \tag{17}$$

Here, $N(t)$ represents the total population of electron-hole pairs at time t, and $\bar{\nu}_r(t)$ is the average radiative recombination rate of these pairs. Now, actually very few electron-hole pairs recombine at early times. At low temperature most of the recombination is radiative. By considering the extensive time range over which PL is emitted in a-Si:H, Street[1] estimates that less than 10^{-4} of all the radiative recombination occurs during the first 100 nsec. Then we assert that the pair population $N(t)$ in Eq. (17) is not significantly depleted on the time scale of this experiment. This leads to the very important conclusion that the rapid attenuation of the integrated intensity $S(t)$ is associated with a *decrease in the average radiative recombination rate* $\bar{\nu}_r(t)$. In fact, the decay of $S(t)$ does not provide any information about the value of $\bar{\nu}_r(t)$, but depends only on the change in $\bar{\nu}_r(t)$. As an example, if $\bar{\nu}_r(t)$ decreases by 70% in the first 20 nsec, then the integrated emission spectrum will decay by 70%, independent of the magnitude of $\bar{\nu}_r(t)$. Thus it is not necessarily true that the rapid attenuation of the PL emission spectrum is associated with fast recombination rates.

The time-resolved emission spectrum indicates that the average radiative recombination rate decreases rapidly in the first 20 nsec. We proceed to discuss two physical mechanisms that can account for this decrease.

The first mechanism, mechanism (1), is based upon the principle that the electron-hole—pair population has a broad distribution of radiative decay times. In general, the pairs with the shortest decay times will be the first to recombine. This leaves the remaining electron-hole—pair population with a longer average decay time. Thus the average recombination rate can decrease rapidly in a statistical sense, while actually very few pairs have recombined.

In order for mechanism (1) to be feasible, there must be a small number of electron-hole pairs that have decay times of ~ 10 nsec. Such fast decay requires that there be a large amount of electron-hole overlap, which suggests that the pairs are actually excitons. In general, it is not necessary that these excitons have small radii, since the crucial factor in determining the decay rate is the electron-hole overlap, and not the spatial extent of the wave function. For instance, bound excitons in cadmium sulfide have radiative lifetimes of ~ 1 nsec and yet are known to extend over $\sim 10^3$ lattice sites.[32] In the case of a-Si:H, however, there is evidence that the holes are strongly localized.[1,2] Under this condition the excitons would have to be small in order to achieve the electron-hole overlap required for fast decay. We proceed to investigate, with a few simple calculations, whether small bound excitons in a-Si:H can have the short decay times necessary to justify mechanism (1).

Within the context of mechanism (1) the excitons can decay either radiatively or nonradiatively. We will first consider the radiative case. Kivelson and Gelatt[16] have worked out the theory of bound excitons in an amorphous semiconductor. They derived a formula for the radiative recombination rate ν_r which is valid if the hole is localized on a single lattice site,

$$\nu_r=\sqrt{\kappa}\,\frac{32e^2\omega^3 r_h^5}{3\hbar c^3 r_e^3}\ . \tag{18}$$

Here, κ is the static dielectric constant, e is the electronic charge, c is the speed of light, ω is the frequency of the emitted radiation, r_h is the radius of the hole wave function, and r_e is the radius of the electron wave function. We choose arbitrary values of the parameters that are appropriate for describing a small exciton in a-Si:H: $\kappa=12$, $\hbar\omega=1.5$ eV, $r_h=2$ Å, and $r_e=5$ Å. Inserting these values into Eq. (18) yields a radiative decay rate of $\nu_r=0.1\ \text{nsec}^{-1}$. Thus it appears that the radiative recom-

bination of tightly bound excitons can account for the rapid attenuation of the emission spectrum, as has been suggested by Wilson *et al.*[11,15]

It is important to also consider the possibility that a small population of excitons could recombine nonradiatively on a nanosecond time scale. In this case the excitons are not required to have nanosecond radiative lifetimes. However, it is necessary that the excitons have the fastest radiative decay rates among the electron-hole–pair population, so that their removal produces the observed decrease in the average radiative recombination rate.

A possible nonradiative recombination channel is multiphonon emission. A simple expression for the nonradiative recombination rate $\nu_{\rm nr}$ of a bound exciton in *a*-Si:H via multiphonon emission, which is valid when the hole is localized on a single lattice site, is[16]

$$\nu_{\rm nr} \simeq 10^{12}(2r_h/r_e)^3 e^{-n} . \tag{19}$$

Here, n is the number of emitted phonons, given by

$$n \geq E/\hbar\omega_0 , \tag{20}$$

where E is the energy of the exciton and ω_0 is a maximum phonon frequency. In *a*-Si:H the vibrations associated with the stretching of the silicon-hydrogen bond have energies as large as $\hbar\omega_0 \simeq 0.25$ eV.[20] Then, by choosing the reasonable values of $r_h = 2$ Å, $r_e = 10$ Å, and $n = 6$, Eq. (19) yields a nonradiative recombination rate of $\nu_{\rm nr} = 0.15$ nsec^{-1}. This demonstrates that the nonradiative decay of excitons can also account for the observed rapid attenuation of the emission spectrum.

A second possible nonradiative recombination channel is the Auger recombination of an exciton at a defect site. In particular, we envision that an exciton could recombine while transferring its energy to an electron that occupied a midgap state, such as a dangling bond. It is difficult to estimate a typical Auger recombination rate, due to the lack of theoretical understanding of this process in amorphous semiconductors. Thus we propose Auger recombination as a possibility that requires further theoretical investigation.

We now consider a fundamentally different mechanism, mechanism (2), that can account for the observed rapid decrease in the average radiative recombination rate. This is simply that the electron and hole wave functions tend to separate on a nanosecond time scale. The average radiative recombination rate decreases because the radiative-transition matrix element is sensitive to the overlap of the electron and hole wave functions. The wave functions can separate either because the electron-hole pairs diffuse apart, or because the pairs relax into more strongly localized states. Note that mechanism (2) can account for the significant decay of the emission spectrum on the nanosecond time scale *without* invoking the existence of excitons with short lifetimes.

An attractive feature of mechanism (2) is that the separation of the electron and hole wave functions can be readily incorporated into the concept of thermalization presented earlier. We believe that the electron-hole pairs thermalize into lower-energy states on the nanosecond time scale. In this process the pairs will tend to either diffuse together or diffuse apart. Let us first consider the possibility that the electron-hole pairs diffuse apart.

The electron and hole wave functions will certainly separate if the electrons and holes tend to diffuse apart as they thermalize into lower-energy states. The diffusion process depends upon the strength of the Coulomb interaction $V_{e\text{-}h}$ between the electrons and holes. It is common to introduce the concept of a critical electron-hole separation r_c, defined as the distance at which the Coulomb energy is equal to the thermal energy,[33,34]

$$V_{e\text{-}h}(r_c) = kT , \tag{21}$$

where k is Boltzmann's constant and T is the temperature. If the average separation of the electrons and holes is less than r_c, then the pairs will tend to diffuse together; otherwise, the pairs will diffuse apart. Clearly, the issue focuses upon the nature of the Coulomb interaction. In *a*-Si:H it is likely that the Coulomb interaction between an electron and hole is small on account of screening. The dielectric constant $\kappa \simeq 12$ indicates that there is considerable electronic screening. There should also be additional screening associated with the deformation of atoms around the strongly localized hole. Screening by the lattice can actually produce an effective Coulomb interaction between the electron and hole that is repulsive.[35] Hence it seems possible that, even at low temperature ($T = 20$ K), the electron-hole pairs diffuse apart as they thermalize on the nanosecond time scale.

Two groups have previously suggested the opposite behavior, that is, at low temperatures the electron and hole tend to diffuse towards each other. Tsang and Street[2] originally proposed this concept in order to explain the increase in the cw PL intensity they observed as the temperature was increased from 2 to 50 K. More recently, however, Street[36] has shown that the increase in the cw PL intensity depends upon the excitation density and is attributable to Auger recombination involving two electron-hole pairs. In any case, we observe no increase in the cw PL intensity with increasing temperature (see Fig. 9).

Collins and Paul[10] have suggested that the average separation of the electron and hole decreases at times less than ~ 25 nsec and then increases at later times. They have measured time-resolved PL emission spectra in sputtered *a*-Si:H, and they propose that the rapid shift of the spectrum to lower energy in the first 25 nsec arises from the increasing Coulomb interaction associated with closer pairs. We have already presented an explanation of the rapid shift of the emission spectrum in terms of the thermalization of the pair population. Hence we feel that there is no direct experimental evidence to suggest that the electron-hole pairs diffuse together at low temperature. It is important to point out, however, that the separation of the electron and hole wave functions, which is the basis of mechanism (2), can still occur in the case where the electron-hole pairs diffuse together as they thermalize. This is because the states that are at lower energy tend to be more strongly localized. Then it is conceivable that the average electron-hole overlap can decrease, even when the electrons and holes diffuse towards

each other, due to an increasing localization of the wave functions.

We have presented two mechanisms that are consistent with the observation that the emission spectrum attenuates rapidly in the nanosecond time regime:

(1) There is a small population of excitons that have either radiative or nonradiative lifetimes on the order of ~ 10 nsec.

(2) The electron and hole wave functions separate on the nanosecond time scale. The separation could result from either an actual diffusion apart of the electron-hole pairs, or an increasing localization of the wave functions as the electrons and holes thermalize into lower-energy states.

Unfortunately, the results of this experiment cannot distinguish between these mechanisms, so that we are unable to unambiguously determine the relevant kinetical process. It is possible that both mechanisms are important.

E. Kinetics of electron-hole pairs at high temperature

The investigation of PL decay as a function of temperature showed that the decay rate significantly increases with temperature. This is quantitatively characterized by the decrease in the decay time cutoff τ_0 (see Fig. 11), which represents a thermal enhancement of the fast decay components. The temperature dependence of τ_0 is found to be well described by

$$1/\tau_0 = \nu_1 + \nu_0 \exp(T/T_0) \,. \tag{14}$$

The physical significance of this relationship is not clear. It has been suggested that the nonradiative-decay rate can have an exponential temperature dependence if the decay mechanism involves tunneling between parabolic minima of the internal potential.[37] An alternative explanation of the temperature dependence described by Eq. (14) has been proposed by Collins and Paul.[38] They show that an exponential temperature dependence can arise if there is a broad distribution of activation energies associated with the nonradiative-decay process.

The essential feature of Eq. (14) is that it describes the same temperature dependence as is observed for the cw PL intensity (Fig. 12). The linear relationship between τ_0 and I_{cw} as a function of temperature conclusively demonstrates that the thermally enhanced decay rate is associated with a nonradiative process. Tsang and Street[2] proposed that the nonradiative-decay mechanism is the diffusion of the electron away from the hole, with subsequent nonradiative recombination at a dangling-bond defect state. A mathematical formulation of this model has been developed[8] which seems able to satisfactorily reproduce the experimentally measured PL decay.

In the preceding section we suggested that at low temperature (20 K) the electron-hole pairs make transitions into lower-energy states on the nanosecond time scale. We believe that at higher temperatures ($T \gtrsim 50$ K) the mobility of the electrons and holes within the localized states increases due to the onset of phonon-assisted transitions. Specifically, an electron (or hole) can either tunnel or hop between localized states more readily by absorbing a phonon. The increased mobility has two important consequences. First, since the transition probabilities between localized states are larger, the electron-hole—pair population thermalizes more rapidly into lower-energy configurations. This increase in the thermalization rate is evident in the behavior of the time-resolved emission spectrum: The shift of the emission spectrum to lower energy is accelerated at higher temperatures (Fig. 13). As discussed earlier, the PL decay measured at a particular emission energy is sensitive to the depletion of the electron-hole—pair population at that energy via thermalization of the pairs into lower-energy states. Hence the thermally enhanced nonradiative decay that is observed on the nanosecond time scale can be attributed to an increase in the thermalization rate of the pair population.

The other effect of the increased mobility at higher temperature is that the spatial diffusion of the electrons and holes is enhanced. In particular, we adopt the interpretation that the electron diffuses away from the more strongly localized hole. Then the electron is more likely to be captured at a midgap state (for example, a dangling bond) before radiative recombination can occur. These states are known to act as nonradiative recombination centers,[1] and this accounts for the quenching of photoluminescence that is observed as the temperature increases above ~ 50 K.

Thus we propose that at temperatures greater than ~ 50 K the mobility of the electrons and holes increases due to the activation of phonon-assisted transitions between the localized states. The increased mobility accelerates the thermalization of the electron-hole pairs into lower-energy states, and also promotes the separation of the electrons and holes by diffusion.

VI. CONCLUSION

Photoluminescence decay in a-Si:H has been measured in the time regime of 0.5—40 nsec as a function of temperature, excitation energy, and emission energy. These measurements represent the first comprehensive energy-resolved study of PL decay in a-Si:H at such early times. The results of this investigation, along with the previous studies of PL decay, provide a substantial basis for understanding the recombination kinetics of electron-hole pairs in a-Si:H. We incorporate these ideas into the following qualitative description of the kinetics of electron-hole pairs on the nanosecond time scale.

When electron-hole pairs are photogenerated, they thermalize within a few picoseconds into the localized band-tail states. The thermalization process is considered to be a type of random walk in which the electrons and holes tend to diffuse apart. However, due to the low mobility of the particles, the electrons and holes are constrained to occupy localized states close to the point in space where they were created, and hence they exist as geminate pairs. The initial separation of the pairs is described by a probability distribution that depends on the excitation energy. At higher excitation energy the width of the distribution increases, so that an electron and hole are less likely to be localized on nearby sites. After the in-

itial thermalization into the band-tail states, we assume that the hole occupies a strongly localized state, and is possibly self-trapped through a lattice deformation. The electron is generally less localized. There could be, however, a few tightly bound excitons that have lifetimes as short as ~ 10 nsec.

The electron-hole pairs continue to thermalize into lower-energy states on the nanosecond time scale. At low temperature the electrons and holes must tunnel between localized states and thermalize by spontaneously emitting phonons. The Coulomb interaction between the electron and hole is expected to be small on account of screening. Then it is possible that, even at low temperature ($T \simeq 20$ K), the electron-hole pairs diffuse apart as they thermalize. At temperatures greater than 50 K the mobility of the electrons and holes is significantly enhanced due to the activation of phonon-assisted transitions between the localized states. The enhanced mobility both increases the rate at which the electron-hole pairs thermalize into the localized states at lower energy and promotes the separation of the electrons and holes by diffusion.

ACKNOWLEDGMENTS

I would like to acknowledge the many friends and associates who have provided encouragement and support throughout this work. In particular, I thank Artie Bienenstock for his continuous support and useful advice. I also thank Bob Street for many enlightening discussions and for providing the samples that were studied in this experiment. This work was supported in part by the National Science Foundation under Contract No. DMR-81-12343, by the U.S. Department of Energy under Contract No. DE-AC03-82ER13000, and by the Danforth Foundation.

APPENDIX: ERROR ANALYSIS

The experimentally measured PL decay was assumed to represent a statistical sampling of some parent distribution. It is well known that the most probable parent distribution can be inferred from the data by the least-squares method. That is, the function that minimizes the sum of the distances between itself and the data points is the most probable representation of the parent distribution. In this case, we assumed that the parent distribution could be described by the function

$$I(t)=a_1+\frac{a_2}{t+\tau_0} . \tag{8}$$

This function, however, did not represent experimentally measured PL decay because there was also error associated with the time coordinate. The error came from two sources. There was uncertainty in the origin of time $t=0$ due to the finite width of the excitation pulse $g(t)$. There was also statistical error in the time coordinate arising from the resolution function $\Gamma(t)$ of the detection system. The most probable distribution describing the experimental PL decay was determined by using the least-squares criteria with the function

$$I'(t)=I(t)*g(t)*\Gamma(t) , \tag{A1}$$

where the asterisk denotes convolution. The quantity $g(t)*\Gamma(t)$ corresponds to the experimentally measured excitation pulse. Thus the analytical procedure was to convolute the experimentally measured excitation pulse with the analytic expression (8) and fit the result, in a least-squares sense, to the experimental PL decay. A minimization routine was used to vary the parameters a_1, a_2, and τ_0 until the best fit was obtained. This analysis provided a method for deconvoluting the PL decay and extracting $I(t)$, the PL decay response to a δ-function excitation. It also yielded values for the decay rate cutoff τ_0 and the quantity $a_1\tau_0/a_2$, which characterize the strengths of the fast and slow decay components, respectively.

The model function (8) was derived in Sec. III A by assuming that the tail of the decay rate distribution could be approximated by an exponential term $\exp(-\tau_0 \nu)$. An informative test of the analytical procedure, and, in particular, the integrity of the model function, was made by varying the time interval over which the PL decay was fitted. The values of τ_0 and $a_1\tau_0/a_2$ obtained by fitting the data set shown in Fig. 2 over different intervals of time after excitation are presented in Fig. 15. It is seen that τ_0 has a constant value of ~ 1.5 nsec until the fitting interval is reduced to less than 10 nsec, at which point the values of τ_0 decrease. This behavior relates to how well the decay rate distribution is approximated by an exponential. If the tail of the distribution was actually an exponential, then τ_0 would be independent of the fitting interval. The fact that τ_0 is relatively constant indicates that the exponential description is reasonable. However the decrease in τ_0 in the earliest time intervals suggests that the tail of the decay rate distribution actually falls off less severely than an exponential.

Since the experimental data exhibit statistical error, it was important to ascertain the error associated with the determination of the quantities τ_0 and $a_1\tau_0/a_2$. The error was estimated in the following way. A computer routine first determined the statistical error in a data set at five points, corresponding to times of 1, 8, 15, 22, and 29 nsec. The parameters a_1, a_2, and τ_0 were then systematically varied away from their optimum values, and the function

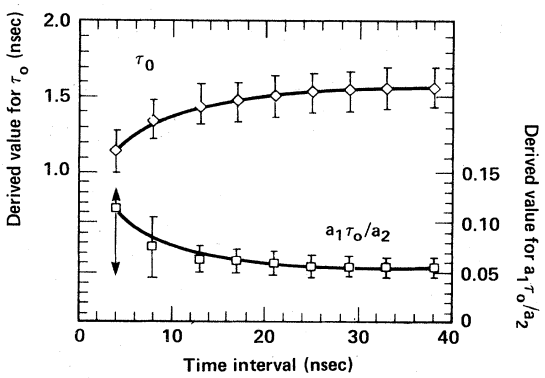

FIG. 15. Dependence of the decay time τ_0 and the quantity $a_1\tau_0/a_2$ on the time interval used in the analysis routine.

$I'(t)$ was calculated at the five times. In this way the parameter space of a_1, a_2, and τ_0 was searched, and a minimum and maximum value of each parameter was found, such that the corresponding $I'(t)$ fell within the statistical-error limits of all five data points. These values of a_1, a_2, and τ_0 were taken to be the error limits in the sense that, for any values of the parameters outside of this range, it would be impossible to find an $I'(t)$ that could reproduce the data within its statistical-error limits.

The same procedure was used to estimate the error in the parameter T_0, which is found in Eq. (14) describing the temperature dependence of τ_0,

$$1/\tau_0=\nu_1+\nu_0\exp(T/T_0)\ . \tag{14}$$

The error in the values of τ_0 was presumably known. Then the parameters ν_1, ν_0, and T_0 were varied about their optimum values, and a minimum and maximum value of T_0 was determined such that the function (14) reproduced the τ_0 values within the error limits.

*Present address: Lawrence Livermore National Laboratory, University of California, P. O. Box 5508, L-473, Livermore, CA 94550.

[1]R. A. Street, Adv. Phys. **30**, 593 (1981).
[2]C. Tsang and R. A. Street, Phys. Rev. B **19**, 3027 (1979).
[3]T. M. Searle, T. S. Nashashibi, I. G. Austin, R. Devonshire, and G. Lockwood, Philos. Mag. B **39**, 389 (1979).
[4]I. G. Austin, T. S. Nashashibi, T. M. Searle, P. G. Le Comber, and W. E. Spear, J. Non-Cryst. Solids **32**, 373 (1979).
[5]S. Kurita, W. Czaja, and S. Kinmond, Solid State Commun. **32**, 879 (1979).
[6]W. Rehm and R. Fischer, Phys. Status Solidi B **94**, 595 (1979).
[7]J. Shah, B. G. Bagley, and F. B. Alexander, Jr., Solid State Commun. **36**, 199 (1980).
[8]K. M. Hong, J. Noolandi, and R. A. Street, Phys. Rev. B **23**, 2967 (1981).
[9]R. W. Collins, P. Viktorovitch, R. L. Weisfield, and W. Paul, Phys. Rev. B **26**, 6643 (1982).
[10]R. W. Collins and W. Paul, Phys. Rev. B **25**, 2611 (1982).
[11]B. A. Wilson, P. Hu, T. M. Jedju, and J. P. Harbison, Phys. Rev. B **28**, 5901 (1983).
[12]D. J. Dunstan, Philos. Mag. B **46**, 579 (1982).
[13]D. J. Dunstan, S. P. Depinna, and B. C. Cavenett, J. Phys. C **30**, L425 (1982).
[14]F. Boulitrop and D. J. Dunstan, Solid State Commun. **44**, 841 (1982).
[15]B. A. Wilson, P. Hu, J. P. Harbison, and T. M. Jedju, Phys. Rev. Lett. **50**, 1490 (1983).
[16]S. Kivelson and C. D. Gelatt, Jr., Phys. Rev. B **26**, 4646 (1982).
[17]T. E. Orlowski, Bull. Am. Phys. Soc. **28**, 239 (1983).
[18]P. Y. Yu and R. S. Berg, Bull. Am. Phys. Soc. **28**, 259 (1983).
[19]J. C. Knights, Jpn. J. Appl. Phys. Suppl. **18**, 101 (1979).
[20]J. C. Knights and G. Lucovsky, CRC Crit. Rev. Solid State Mater. Sci. October issue, 212 (1980).
[21]The value given for the optical band gap is derived from the intercept of a plot of $\sqrt{\alpha\hbar\omega}$ vs $\hbar\omega$, where $\hbar\omega$ is the photon energy and α is the absorption coefficient.
[22]R. A. Street, J. C. Knights, and D. K. Biegelsen, Phys. Rev. B **18**, 1880 (1978).
[23]R. A. Street, Phys. Rev. B **26**, 3588 (1982).
[24]D. G. Stearns, Ph.D. thesis, Stanford University, 1984.
[25]R. W. Collins, M. A. Paesler, and W. Paul, Solid State Commun. **34**, 833 (1980).
[26]R. Fischer, W. Rehm, J. Stuke, and U. Voget-Grote, J. Non-Cryst. Solids **36**, 687 (1980).
[27]E. A. Davis, J. Non-Cryst. Solids **4**, 107 (1970).
[28]J. C. Knights and E. A. Davis, J. Phys. Chem. Solids **35**, 543 (1974).
[29]It is often assumed that the decay rate ν and the electron-hole separation R can be related by $\nu=\nu_0\exp(-2\alpha R)$, where ν_0 and α are parameters that depend upon the detailed nature of the wave functions. This expression, however, is not valid when the overlap of the electron and hole wave functions is large, such that the decay rate is greater than $\sim 10^8$ sec^{-1}, and hence the expression is not applicable in our analysis.
[30]Z. Vardeny and J. Tauc, Phys. Rev. Lett. **46**, 1223 (1981).
[31]N. F. Mott and E. A. Davis, *Electronic Processes in Non-Crystalline Materials* (Clarendon, Oxford, 1979), p. 22.
[32]C. H. Henry and K. Nassau, Phys. Rev. B **1**, 1628 (1970).
[33]D. M. Pai and R. C. Enck, Phys. Rev. B **11**, 5163 (1975).
[34]K. M. Hong and J. Noolandi, J. Chem. Phys. **68**, 5163 (1978).
[35]D. Emin, *Polycrystalline and Amorphous Thin Films and Devices* (Academic, London, 1980), p. 17.
[36]R. A. Street, Phys. Rev. B **23**, 861 (1981).
[37]R. A. Street, T. M. Searle, and I. G. Austin, in *Amorphous and Liquid Semiconductors,* edited by J. Stuke and W. Brenig (Taylor and Francis, London, 1974), p. 953.
[38]R. W. Collins and W. Paul, Phys. Rev. B **25**, 5257 (1982).